Villalonga, R.; Díez, P.; Sánchez, A.; Aznar, E.; Martínez-Máñez, R.; Pingarrón, J. (2013). Enzyme-controlled sensing-actuating nanomachine based on Janus Au-mesoporous silica nanoparticles. Chemistry - A European Journal. 19(24):7889-7894. https://doi.org/10.1002/chem.201300723

CHEMISTRY
A EUROPEAN JOURNAL

FULL PAPER

DOI: 10.1002/chem.200((will be filled in by the editorial staff))

Enzyme-controlled sensing-actuating nanomachine based on Janus Au-mesoporous silica nanoparticles

Reynaldo Villalonga,*[a,b] Paula Díez,[a] Alfredo Sánchez,[a] Elena Aznar,[c,d] Ramón Martínez-Máñez,[c,d] José M. Pingarrón*[a,b]

Dedication ((optional))

Abstract: Novel Janus nanoparticles with Au and mesoporous silica opposite faces were prepared by Pickering emulsion template using paraffin wax as oil phase. These anisotropic colloids were employed to design an integrated sensing-actuating nanomachine for the enzyme-controlled stimulus-responsible delivery of a cargo compound. As a proof-of-concept, we demonstrated the successful use of the Janus colloids for controlled cargo delivery from the mesoporous silica face grafted with pH-sensitive gate-like scaffoldings. The release of the cargo (tris(2,2´-bipyridyl)ruthenium(II) chloride in this case) was mediated by the on-demand catalytic decomposition of urea by urease, which was covalently immobilized on the Au face.

Keywords: Janus nanoparticle, mesoporous silica, molecular gates, controlled release, enzyme

Introduction

The development of novel biologically-inspired nanomachines and smart drug delivery systems is linked to the tailor-made design of advanced nanomaterials with desired physical properties and chemical functionalities.[1] Among these, particular interest has been devoted to the preparation of anisotropic colloidal particles which exhibit two surfaces of different chemical composition.[2] These so-called "Janus nanoparticles" can be designed to show amphiphilic character as well as anisotropic electrical, magnetic or optical properties.[3] Additionally, each face of the Janus nanoparticles can be independently modified with selected ligands allowing specific functionalization with proteins and other biomacromolecules.[4] These unique characteristics have favored the successful use of Janus nanomaterials as emulsion stabilizers, hydrophobic coat for textiles, self-propelled machines, imaging probes, and drug delivery systems.[5]

On a different approach nanotechnology has proved to bring new innovative concepts to drug-delivery therapies. Drug delivery systems able to release active molecules to certain cells in a controlled manner have recently gained much attention. Among several potential drug delivery systems, mesoporous silica nanoparticles (MS) have been widely used in the past years as reservoirs for drug storage due to their unique properties such as a large specific volume, large loading capacity, low toxicity and easy functionalization.[6] Moreover MS nanoparticles can be functionalized with molecular/supramolecular ensembles on their external surface to develop gated-MS showing "zero delivery" and capable to release of their cargo in response to external stimuli. Using this concept, MS displaying controlled release using several stimuli such as pH, light, redox substances, small molecules and biomolecules have been reported.[7] However, a potential limitation in these systems is related with the fact that the delivery MS-based support and the effector (i.e. agent that mediates the delivery) are not in the same nanoparticle and usually the gated materials are placed in a solution in which the triggering stimuli is applied (for instance light) or it is present in the media (for instance enzymes that induced the degradation of a specific gating coating).

As an advance in the design of more sophisticated nanoparticles for delivery applications we envisioned that it might possible to project systems in which the gating systems and an effector molecule could be placed in the same nano-device. In order to achieve this goal the strategy we have followed in shown in

[a] R. Villalonga, P. Díez, A. Sánchez, J.M. Pingarrón
Department of Analytical Chemistry, Complutense University of Madrid
28040-Madrid, Spain , Fax: (+34) 913944329
E-mail: rvillalonga@quim.ucm.es, pingarro@quim.ucm.es

[b] IMDEA Nanoscience, Cantoblanco Universitary City, 28049-Madrid, Spain.

[c] E. Aznar, R. Martínez-Máñez
Departamento de Química and CIBER de Bioingeniería, Biomateriales y Nanomedicina (CIBER-BBN), Universidad Politécnica de Valencia,
Camino de Vera s/n, E-46022, Valencia, Spain , Fax: (+34) 963879349
E-mail: elazgi@upvnet.upv.es, rmaez@qim.upv.es

[d] Instituto de Reconocimiento Molecular y Desarrollo Tecnológico (IDM), Centro Mixto Universidad Politécnica de Valencia-Universidad de Valencia, Spain

Supporting information for this article is available on the WWW under http://www.chemeurj.org/ or from the author.

Scheme 1 and it involves the preparation of new Janus Au-MS nanoparticles by Pickering emulsion template using paraffin wax as oil phase. This allows obtaining two different surfaces with well-defined functionalization chemistries for the independent anchoring of the gated ensemble (on the MS face) and the effector molecule (on the Au face).

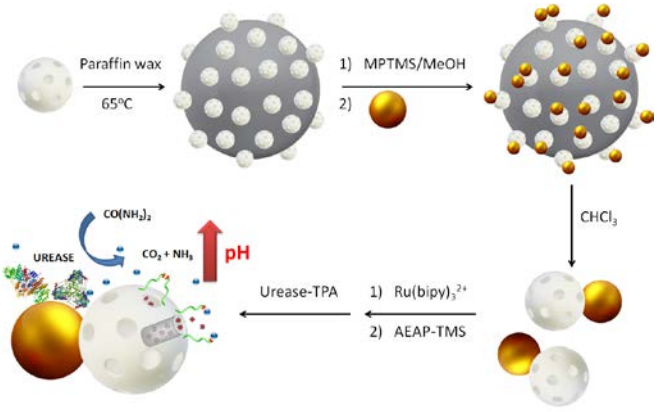

Scheme 1. Preparation of Janus Au-MS nanoparticles for enzyme-controlled release.

In this particular case, and as a first proof-of-concept, the MS part of the anisotropic colloid was capped with a pH-responsive gate, whereas the gold surface was functionalized with the enzyme urease (EC 3.5.1.5). We reasoned that the gated mesoporous nano-devices would show "zero-release", yet selectively will open the pH-responsive gate releasing the cargo in the presence of urea via urease-mediated urea hydrolysis which will lead to an increase of the pH.

Results and Discussion

The starting MS nanoparticles (a calcined MCM41-like solid) were synthesized by alkaline hydrolysis of tetraethyl orthosilicate as inorganic precursor in the presence of the cationic surfactant cetyltrimethylammonium bromide as porogen species.[8] The MS showed an average particle diameter of 97 ± 15 nm and an MCM-41 type channel-like mesoporous structure (Figure 1S in Supporting Information).

To synthesize the Janus nanoparticles, a rational design based on the manipulation of the Au-ligan-MS interface through mask-protecting assisted site-selective modification was employed. First, the surface of MS nanoparticles was partially masked by confining at the interface of Pickering emulsion. The exposed nanoparticle surface was further modified with a thiolated silane derivative, providing reactive sulfhydryl groups on this face. Au nanoparticles were then attached to the thiol-enriched face of the adsorbed MS nanoparticles through chemisorption reactions, forming stable anisotropic colloids. Several anisotropic nanomaterials have been previously prepared in excellent yield by manipulation of nanoparticle-ligand-nanoparticle interfaces in solutions.[9] In the present work, such toposelective manipulation was performed in a solid-liquid interface.

According to this synthetic scheme, the as-prepared MS were first adsorbed onto the liquid-liquid interface of an emulsion prepared with water and molten paraffin wax, forming colloidosomes that remained stable after cooling.[10] Although the formation of such colloidosomes was previously reported using silica nanoparticles with average diameters larger than 400 nm,[10,11] we have proved here that this procedure can also be also used using MS nanoparticles of smaller diameter.

The toposelective modification of the MS nanoparticles adsorbed onto the colloidosome surface was performed by reaction with (3-mercaptopropyl)trimethoxysilane in water:methanol solution. After exhaustive washing, the colloidosomes containing the thiol-functionalized MS nanoparticles were stirred in Au nanoparticles solution. Janus Au-MS nanoparticles were finally obtained with acceptable yield (about 85% for J2 sample) after dissolving the paraffin wax in $CHCl_3$.

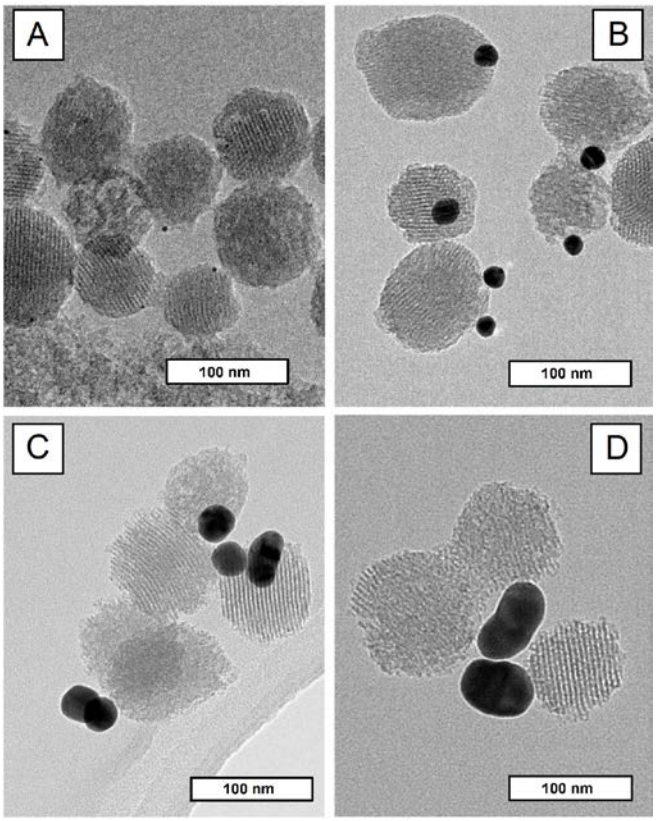

Figure 1. TEM images of J1 (A), J2 (B), J3 (C) and J4 (D) Janus Au-MS nanoparticles.

Figure 1 shows the TEM images of Janus colloids prepared by using Au nanoparticles of different sizes: 3.7 ± 0.8 nm (J1),[12] 20 ± 2 nm (J2), 31 ± 6 nm (J3) and 43 ± 5 nm (J4).[13] In all cases, anisotropic colloids were successfully synthesized, mainly with a 1:1 Au:MS nanoparticles ratio except for J1 samples in which the use of smaller Au nanospheres favored the attachment of more than one metal nanoparticle to the same MS colloid. J1 nanoparticles showed similar average diameter (98 ± 17 nm) and size distribution than the native MS colloid, with only slight difference at higher values of diameter (Figure 2S in Supporting Information). This fact can be justified by the small diameter and low polydispersity of the attached Au nanoparticles. Moreover, J1 anisotropic colloids showed low metal content, which should be counterproductive for the further immobilization of urease and the preparation of the enzyme-controlled nanomachines.

Large average diameter and broad size distribution was observed for J3 (117 ± 19 nm) and J4 (126 ± 23 nm) nanoparticles. This could be ascribed to the large diameter and size dispersion of Au nanoparticles prepared by Frens method using low citrate concentration,[13] which often yield nanoparticles with non-spherical shape. In J4 samples, prepared using large Au nanoparticles,[13] it was observed that some Au nanoparticles were assembled to more than one MS nanoparticle, yielding aggregated structures. This fact could be justified by the close packing of the MS nanoparticles onto the colloidosome surface, allowing the interaction of several thiol-modified mesoporous colloids with the same large and non-spherical

Au nanoparticle. It should be highlighted that sample J2 (104 ± 17 nm) showed narrow distribution of size and maximum yield of Au-MS anisotropic nanoparticles with 1:1 ratio, and accordingly this Janus colloid was selected for further experiments. A representative TEM image corresponding to J2 nanoparticles is shown in Figure 2. Other different TEM images of J2 nanoparticles are also shown in Figure 3S in Supporting Information.

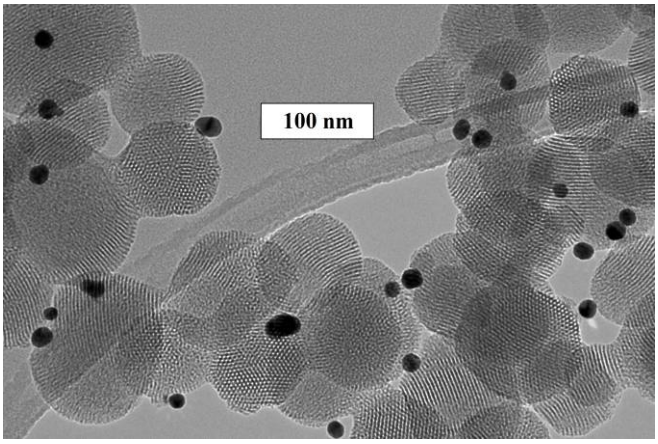

Figure 2. Representative TEM image of J2 nanoparticles.

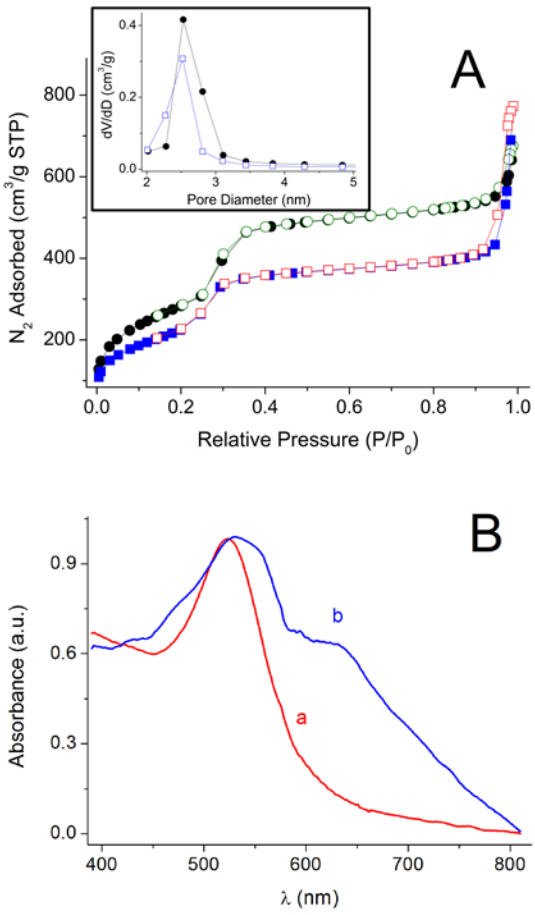

Figure 3. A) Nitrogen adsorption (closed)/desorption (open) isotherms for MS (●,○) and J2 nanoparticles (■,□). Inset: pore size distribution of MS (●) and J2 (□) nanoparticles. B) Normalized visible spectra of Au (a) and J2 (b) nanoparticles.

The pore morphologies of the MS and Janus Au-MS nanoparticles in the J2 nanoparticles were determined by nitrogen adsorption/desorption surface analysis (BET isotherms and BJH pore size distributions). Figure 3A illustrates the corresponding nitrogen adsorption/desorption isotherms and the pore size distributions for the starting MS material and for the corresponding J2 Janus nanoparticles. Both nanomaterials showed type IV isotherms typical of mesoporous supports.

The absence of hysteresis loops for MS nanoparticles suggested that all pores are highly accessible. On the contrary, the small hysteresis loops observed at high relative pressure values in the Janus nanoparticle isotherm suggested that some pores were partially blocked most likely due to the toposelective silanization with (3-mercaptopropyl)trimethoxysilane and the attachment of the Au nanoparticles. In fact the attachment of Au nanoparticles on one face of the siliceous matrix reduced the BET specific surface area from 1037 m²/g in the starting MS to 820 m²/g in J2. Yet the average pore size of the MS support (ca. 2.5 nm) was unchanged after formation of the anisotropic colloid (see inset of Figure 3A).

UV-vis measurements in aqueous solutions were performed to provide insight into the surface characteristics of the Janus nanoparticles (Figure 3B). The starting Au colloids showed a single absorption band at 522 nm, distinctive of the surface plasmon resonance of spherically-shaped nanospheres with about 20 nm diameter, whereas the attachment of the Au nanoparticles to the thiol-modified MS nanoparticles leads to a broadening and red-shift of the plasmon band in the J2 spectra. In addition, a broad shoulder band from 585 nm to 630 nm was also observed in the spectrum of J2 which can be tentatively attributed to the attachment of more than one Au nanospheres on the surface of the MS nanoparticles in some Janus particles, causing a coupling of the plasma modes due to metal particle-particle interactions.[14]

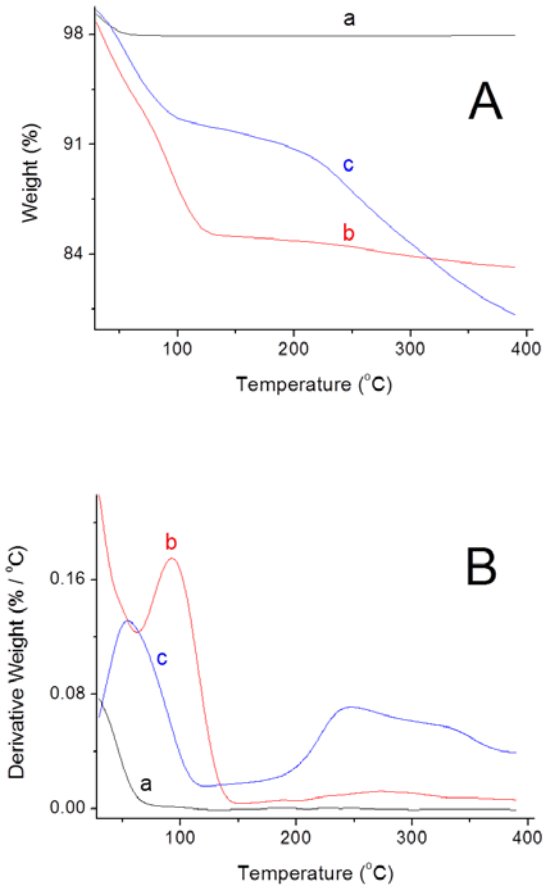

Figure 4. A) TG and B) DTG analysis for MS (a), J2 (b) and J2Ru (c) nanoparticles.

J2 colloid was further employed as nanosized hardware for the assembly of a self-controlled nanomachine able to release a cargo compound by an enzyme-based pH-mediated mechanism. In a first step J2 nanoparticles were loaded with tris(2,2´-bipyridyl)ruthenium(II) chloride ($[Ru(bpy)_3]^{2+}$) as model dye for monitoring cargo delivery.[7c] Thereafter, an excess of the alkyl amino derivative 3-(2-aminoethylamino)propyltrimethoxysilane (the pH-responsive molecular gate) was anchored on the external surface of the mesoporous face to yield the J2Ru nanomaterial.[7a] It should be mentioned that Janus nanoparticles exhibited good water solubility, but its stability in aqueous solutions was reduced after modification with 3-(2-aminoethylamino)propyltrimethoxysilane.

Thermal analysis of the MS, J2 and J2Ru nanomaterials was accomplished, the TG/DTG curves being displayed in Figures 4 (A,B). The unmodified MS nanoparticles exhibited a slight weight loss at temperatures up to ca. 70ºC, which was attributed to the thermodesorption of physically adsorbed water molecules from the silica surface. At higher temperatures no weight loss was apparent showing relatively flat TG/DTG curves.[15] Janus nanoparticles showed a more noticeable weight loss at temperatures up to ca. 140ºC suggesting that higher amount of water molecules were adsorbed on the Au nanoparticles surface. The anisotropic nanoparticle exhibited a second thermal-induced transformation, with maximum rate of weight loss at approximately 275ºC, which could be associated with the decomposition of the bonded thiol ligands but also with the condensation of the ligand's side silanols with one another or with surface silanols.

In comparison with J2, the weight loss profile for J2Ru exhibited a lower decrease at T < 120ºC, suggesting lower amount of water molecules physically adsorbed on this nanomaterial. This fact could be justified by the azeotropic treatment of the Janus nanoparticles before adsorption of the $[Ru(bpy)_3]^{2+}$ complex and silanization with 3-(2-aminoethylamino)propyltrimethoxysilane, as well as to the introduction of the long chain aminosilane groups on the MS face. The weight loss at higher temperatures can be divided into two regions. The first region, with maximum rate of weight loss at 245ºC, could be attributed to decomposition/condensation of the bounded ligands. The second thermal-induced process, which showed a maximum rate of transformation at about 330ºC, could be associated with the decomposition of the $[Ru(bpy)_3]^{2+}$ complex, which is thermally stable up to 320 °C.[16] The loading of the $[Ru(bpy)_3]Cl_2$ dye in the J2Ru material amounted to 62 mg/g J2Ru in weight, as determined by the TG curve. Moreover the content of the anchored amine-based gate amounted to 49 mg/ g J2Ru in weight.

Figure 5A shows an FT-IR spectrum of the MS, J2 and J2Ru nanoparticles. MS nanoparticles showed the characteristics IR absorption bands of siliceous materials at 456 cm^{-1} attributed to the vibration of the Si-O bonds, a shoulder at 576 cm^{-1} ascribed to cyclic Si-O-Si structures, at 803 cm^{-1} attributed to SiO_4 tetrahedrons, at 946 cm^{-1} attributed to the Si-OH groups, and a band at 1080 cm^{-1} with a shoulder at 1200 cm^{-1} ascribed to the bond stretching vibrations of Si-O-Si.[17] The broad band at 3700-3000 cm^{-1} can be ascribed to the O-H bonding vibration of adsorbed water and SiO-H groups, and the band at 1629 cm^{-1} is attributed to the deformation vibration of the HO-H bond in water molecules.

Spectrum of J2 nanoparticles presented the antisymmetric and symmetric stretching vibrations of the CH_2 groups at 2933 cm^{-1} and 2856 cm^{-1}, confirming the modification of the MS nanomaterial with (3-mercaptopropyl)trimethoxysilane. The absence of the characteristic bands of S-H vibration in the range of 2500-2600 cm^{-1} suggested that the thiol groups were chemisorpted to the Au nanoparticle surface. Loading of J2 with $[Ru(bpy)_3]^{2+}$ and derivatization with 3-(2-aminoethylamino)propyltrimethoxysilane was further confirmed by the bands at 2946 cm^{-1} and 2859 cm^{-1} ($\upsilon_{[C-H]}$), 1633 cm^{-1} ($\delta_{[N-H]}$), 1568 cm^{-1} ($\upsilon_{[C-C]} + \upsilon_{[C=C-H]}$), 1480 cm^{-1} ($\upsilon_{[C-C]} + \upsilon_{[C=C-H]}$) and 1319 cm^{-1} ($\upsilon_{[NC-H]}$) in the J2Ru spectrum.[18] Another important characteristic is the drop in intensity of the band around 950 cm^{-1}, which is attributed to the vibration of the silanol groups, confirming the modification of the mesoporous silica surface with the amine-bearing silane.[7a]

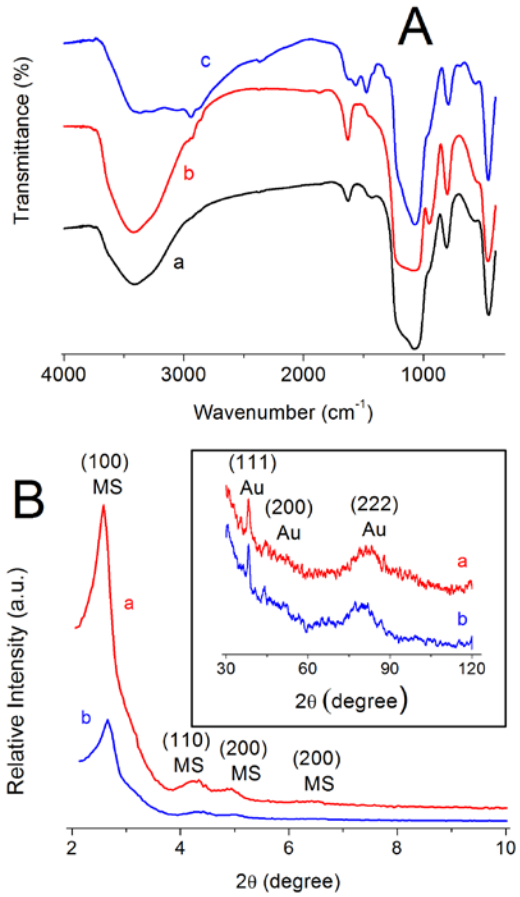

Figure 5. A) FT-IR analysis for MS (a), J2 (b) and J2Ru (c) nanoparticles. B) X-ray diffraction of J2 (a) and J2Ru (b) nanoparticles.

The powder X-ray diffraction patterns of J2 and J2Ru are shown in Figure 5B. The low angle diffractogram of J2 shows four distinguishable peaks at 2.59º, 4.30º, 4.93º and 6.46º which correspond to (100), (110), (200) and (210) of MCM-41 with d-spacing values of 3.40 nm, 2.05 nm, 1.79 nm and 1.37 nm, respectively. This pattern suggested perfect long-range order in this mesoporous nanomaterial. Additionally, from these data and the pore value diameter obtained from nitrogen adsorption isotherms, an a_0 cell parameter of 3.93 nm and a pore wall thickness of 1.40 nm can be calculated. Moreover, the diffraction pattern of J2 at high angle showed three peaks at 38.34º, 44.50º and 81.21º, corresponding to the (111), (200) and (222) Bragg reflections for cubic gold nanocrystals,[19] confirming the Janus architecture previously observed by TEM. J2Ru sample showed similar X-ray diffraction pattern, suggesting that the loading process with the dye and the further functionalization with amine groups did not damage neither the mesoporous MCM-41 type structure nor of the gold face of the Janus colloid.[7c]

In order to prepare the self-controlled enzyme-powered nanodevice for cargo delivery, the Au face of the Jan2Ru nanoparticles were functionalized with the enzyme urease. For

preparing an enzyme form suitable to be anchored on the metal surface, urease was covalently modified with 3,3´-dithiobis(sulfosuccinimidylpropionate) (DTSSP). After reduction of the dithiol linkage with $NaBH_4$, the modified enzyme solution was dialyzed and finally incubated with J2Ru to yield the J2Ru-U nanomaterial. All these processes were performed in 50 mM sodium phosphate buffer, pH 7.0, at 4ºC.

The ability of J2Ru-U nanoparticle to deliver the $[Ru(bpy)_3]^{2+}$ dye under urease control was tested in 5 mM sodium acetate buffer at pH 4.0 and 5.0. It is well know that the pH-activity profile of urease has a bell-shaped behavior with maximum at pH 7.0.[20] However, more than 66% of the 3-(2-aminoethylamino) propyltrimethoxysilane grafting moieties on the MS surface are unprotonated at this pH value,[7a] then the gate-like ensembles was partially open. To avoid this undesirable effect, we used buffer solution of pH 5.0 where urease retains about 60% of its maximum catalytic activity,[20] and not appreciable release of the dye from J2Ru-U was experimentally observed in the control experiments.

In a typical release assay, 10 mg of J2Ru-U were suspended in 10 mL of buffer solution containing 180 mM urea, and shaken over time at 25ºC. Aliquots were taken at scheduled times, centrifuged and the absorbance was measured at 454 nm. As control experiments, J2Ru-U samples were suspended in similar buffer solution without urea. In order to ensure saturating conditions for substrate in the enzyme catalyzed reaction, concentration of urea about 100-fold larger than K_M = 1.3 mM was employed.

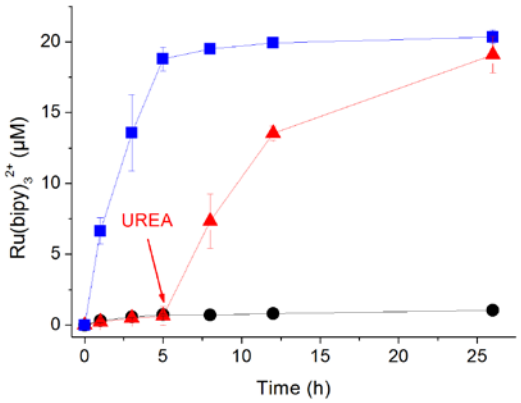

Figure 6. Kinetics of dye release from J2Ru-U in 5 mM sodium acetate buffer pH 5.0 in the absence (●) and the presence of 180 mM urea at t = 0 (■) or t = 5 h (▲).

Figure 6 shows the time-course of $[Ru(bpy)_3]^{2+}$ release from the pores of the J2Ru-U nanoparticles. The concentration of dye delivered to the solution increased progressively with the time of incubation for the mixture containing urea at pH 5.0, reaching plateau value of about 19 μM after 5 h of incubation. On the contrary, no significant increase in the absorbance measured at 454 nm was observed for control solution containing no urea.

Urease catalyzed the transformation of urea to CO_2 and NH_3 yielding a progressive increase in the pH value of the incubation solutions, as it was qualitatively demonstrated by adding bromothymol blue to control assays. As it was previously reported, the 3-(2-aminoethylamino)propyltrimethoxysilane moieties located on the MS surface became gradually deprotonated when the solution pH reached alkaline values.[7a] Consequently, the nanoscopic molecular gates located at the pore outlets trended to be opened favoring the release of the dye.

To provide insight into this enzyme-controlled dye release mechanism, J2Ru-U nanomaterials were incubated in buffer solution without urea under the conditions described above. Urea (180 mM final solution) was then added after 5 h of incubation, the results being shown in Figure 6. No appreciable dye release was observed during the first 5 h of incubation but the further increase in the absorbance at 454 nm revealed that the dye was successfully delivered to the solution after adding urea.

Conclusion

In summary, we described the preparation of Janus-type nanoparticles having Au and MS opposite faces and have used them for the design of an integrated nano-device containing on the same nanoparticle a gating systems and an effector molecule for the stimulus-responsible delivery of a cargo. In this particular case, as a proof-of-concept the release was mediated by the on-demand catalytic decomposition of urea by the enzyme urease, which was immobilized on the Au face, whereas the gated ensemble consisted of a pH-responsive system which was anchored on the pore outlets of the MS phase. In spite of the many reports dealing with the preparation of silica-based anisotropic colloids, approaches to produce MS-based Janus nanoparticles and their evaluation as on-demand control release systems are scarce to our knowledge. We believe that the possibility of incorporate different effector molecules and gated ensembles on this Janus-type integrated nanoarchitecture, which constitutes a proof-of-concept, open new routes for the development of novel biologically-inspired smart nanomachines for drug delivery and sensing applications and research is this line is currently being performed by us.

Experimental Section

Preparation of MS nanoparticles:[8] Cetyltrimethylammonium bromide (3.0 g) was dissolved in 1.44 L of water under sonication. NaOH solution (2.0 mol/L, 10.5 mL) was then added and the temperature of the mixture was adjusted to 80 ºC. Tetraethoxysilane (15.0 mL) was added dropwise to the surfactant solution within 5 min under vigorous magnetic stirring. The mixture was allowed to react for 2 h. The resulting white solid was filtered, washed with water and methanol, and then dried in desiccator. The solid was finally calcinated at 550 ºC for 5 h.

Preparation of 3.7 nm Au nanoparticles:[12] An ice-cold, freshly prepared 0.1 M $NaBH_4$ solution (600 μL) was quickly added to 20 mL aqueous solution containing 300 μM $HAuCl_4$ and 300 μM trisodium citrate under continuous stirring. The mixture was stirred for 30 min, and 100-fold diluted with 300 μM trisodium citrate before J1 preparation.

Preparation of 18 nm, 29 nm and 41 nm Au nanoparticles:[13] Freshly prepared 3 μM $HAuCl_4$ solutions (50 μL) were heated to boiling. Au nanoparticles of 18 nm, 29 nm and 41 nm were synthesized by adding 750 μL, 500 μL and 300 μL of 3.9 μM trisodium citrate solution, respectively. The mixtures were heated for 10 min, cooled to room temperature and finally raised to 50 mL with ultrapure water.

Preparation of Janus Au-MS nanoparticles: Janus nanoparticles were synthesized by adapting two methods previously reported in literature.[10] MS nanoparticles (200 mg) were dispersed homogeneously in 10 mL of 1.0 μM of CTAB in 6.7% ethanol aqueous solution. The mixture was heated at 75ºC and then 1 g of paraffin wax was added. When the paraffin wax was melted, the mixture was vigorously mixed at 25000 rpm during 2 min using an Ultra-Turrax T-10 homogenizer (IKA, Germany). The resulting emulsion was further mixed during 5 min at 4000 rpm and 75 ºC, using the same apparatus. The resulting Pickering emulsion was then cooled to room temperature, mixed with 10 mL methanol and treated with 200 μL of (3-mercaptopropyl)trimethoxysilane. After 3 h under magnetic stirring, the silanized emulsion was filtered, three-times washed with methanol and further dispersed in 400 mL of the corresponding 3 μM Au nanoparticles aqueous solutions. The mixture was stirred overnight, then filtered and exhaustively washed with ultrapure water. The solid was suspended in ethanol, centrifuged and washed two-times with ethanol and three-times with chloroform. The Janus nanoparticles were finally dried and kept in dissecator until use.

Preparation of J2Ru-U: To synthesize J2Ru, 100 mg of J2 and 60 mg of tris(2,2´-bipyridyl)ruthenium(II) chloride hexahydrate were suspended in 10 mL of anhydrous

acetonitrile inside a round-bottom flask connected to a Dean-Stark trap under Ar atmosphere.[7a] The suspension was refluxed at 110 °C in azeotropic distillation, collecting about 4 mL in the trap in order to remove the adsorbed water. The mixture was stirred for 24 h at room temperature to load the dye into the MS face pores. Afterward, an excess of 3-(2-aminoethylamino)propyltrimethoxysilane (500 µL) was added, and the suspension was stirred for 5.5 h. Finally, the orange solid (J2Ru) was filtered off, washed two times with 30 mL of CH_3CN, and dried at 70 °C for 12 h.

To synthesize J2Ru-U, 4.0 mg of urease and 4.0 mg of 3,3´-dithiobis(sulfosuccinimidylpropionate) were dissolved in 5.0 mL of 50 mM sodium phosphate buffer, pH 7.0, and stirred during 2 h at 4 ºC. Afterward, 200 µL of 100 mM $NaBH_4$ solution were added, and the mixture was stirred at 4 ºC for 30 min. The solution was exhaustively dialyzed *vs.* 50 mM sodium phosphate buffer, pH 7.0 using Amicon Ultra-05 centrifugal filter units with Ultracel-10 membranes (Millipore, USA), and finally concentrated to about 10 mg/mL concentration. The modified enzyme solution was then added to 50 mL sodium phosphate buffer, pH 7.0, containing 50 mg of J2Ru, and stirred at 4ºC overnight. The resulting solid (J2Ru-U) was finally isolated by centrifugation, washed several times with sodium phosphate buffer, pH 7.0, dried and kept in refrigerator until use.

Characterization: Transmission electron microscopy (TEM) measurements were performed with JEOL JEM-3000 F and JEOL JEM-2100 microscopes. The morphology of the colloidosomes was characterized using high resolution field emission scanning electron microscopy (FE-SEM) with a JEOL JSM-6335F electron microscope (JEOL Ltd., Japan). FT-IR spectra were acquired with a Perkin-Elmer instrument. Spectrophotometric measurements were performed using an Agilent 8453 UV/VIS spectrophotometer (Hewlett Packard, USA). Power X-ray diffraction (XRD) was performed with an X'Pert MRD diffractometer (PANanalytical B.V., The Netherlands). Nitrogen adsorption/desorption isotherms and pore size distributions were determined with an ASAP 2020 Physisorption Analyzer (Micromeritics, USA). Thermal analysis was performed with a TA Instruments SDT-Q600 apparatus (USA). FT-IR spectra were acquired with a Nicolet Nexus 670/870 spectrometer (Thermo Fisher Scientific Inc., USA).

Acknowledgements

R. Villalonga acknowledges to Ramón & Cajal contract from the Spanish Ministry of Science and Innovation. Financial support from the Spanish Ministry of Science and Innovation CTQ2011-24355, CTQ2009-12650, CTQ2009-09351, MAT2009-14564-C04-01, MAT2012-38429-C04-01 and Comunidad de Madrid S2009/PPQ-1642, programme AVANSENS is gratefully acknowledged. The Generalitat Valencia (project PROMETEO/2009/016) is also acknowledged.

[1] N. Hasirci, in *Nanomaterials and Nanosystems for Biomedical Applications* (Ed.: M.R. Mozafari), Springer, Germany, **2007**.

[2] a) A. Perro, S. Reculusa, S. Ravaine, E. Bourgeat-Lami, E. Duguet, *J. Mater. Chem.* **2005**, *15*, 3745; b) S. Jiang, Q. Chen, M. Tripathy, E. Luijten, K.S. Schweizer, S. Granick, *Adv. Mater.* **2010**, *22*, 1060.

[3] M. Lattuada, T.A. Hatton, *Nano Today* **2011**, *6*, 286.

[4] J.L. Tang, K. Schoenwald, D. Potter, D. White, T. Sulchek, *Langmuir* **2012**, *28*, 10033.

[5] a) J.W. Kim, D. Lee, H.C. Shum, D.A. Weitz, *Adv. Mater.* **2008**, *20*, 3239; b) A. Synytska, R. Khanum, L. Ionov, C. Cherif, C. Bellmann, *ACS Appl. Mater. Interfaces* **2011**, *3*, 1216; c) J.R. Howse, R.A. Jones, A.J. Ryan, T. Gough, R. Vafabakhsh, R. Golestanian, *Phys. Rev. Lett.* **2007**, *99*, 048102; d) M. Yoshida, K.H. Roh, J. Lahann, *Biomaterials* **2007**, *28*, 2446; e) A.K. Salem, P.C. Searson, K.W. Leong, *Nat. Mater.* **2003**, *2*, 668.

[6] a) L. Zhang, F. Zhang, W.F. Dong, J.F. Song, Q.S. Huo, H.B. Sun, *Chem. Commun.* **2011**, *47*, 1225; b) J.E. Lee, N. Lee, T. Kim, J. Kim, T. Hyeon, *Acc. Chem. Res.* **2011**, *44*, 893.

[7] a) R. Casasús, E. Climent, M.D. Marcos, R. Martínez-Máñez, F. Sancenón, J. Soto, P. Amorós, J. Cano, E. Ruiz, *Am. Chem. Soc.* **2008**, *130*, 1903; b) A. Bernardos, L. Mondragón, E. Aznar, M.D. Marcos, R. Martínez-Máñez, F. Sancenón, J. Soto, J.M. Barat, E. Pérez-Payá, C. Guillem, P. Amorós, *ACS Nano* **2010**, *4*, 6353; c) I. Candel, A. Bernardos, E. Climent, M.D. Marcos, R. Martínez-Máñez, F. Sancenón, J. Soto, A. Costero, S. Gil, M. Parra, *Chem. Commun.* **2011**, *47*, 8313.

[8] Y. Zhao, B.G. Trewyn, I.I. Slowing, V.S.Y. Lin, *J. Am. Chem. Soc.* **2009**, *131*, 8398.

[9] Y. Feng, J. He, H. Wang, Y.Y. Tay, H. Sun, L. Zhu, H. Chen, *J. Am. Chem. Soc.* **2012**, *134*, 2004; T. Chen, G. Chen, S. Xing, T. Wu, H. Chen, *Chem. Mat.* **2010**, *22*, 3826.

[10] L. Hong, S. Jiang, S. Granick, *Langmuir* **2006**, *22*, 9495; A. Perro, F. Meunier, V. Schmitt, S. Ravaine, *Colloids Surf. A* **2009**, *332*, 57.

[11] D. Rodríguez-Fernández, J. Pérez-Juste, I. Pastoriza-Santos, L.M. Liz-Marzán, *ChemistryOpen* **2012**, *1*, 90.

[12] N.R. Jana, L. Gearheart, C.J. Murphy, *Langmuir* **2001**, *17*, 6782.

[13] G. Frens, *Nature* **1973**, *241*, 20.

[14] S.K. Ghosh, T. Pal, *Chem. Rev.* **2007**, *107*, 4797.

[15] a) C.P. Jaroniec, M. Kruk, M. Jaroniec, A. Sayari, *J. Phys. Chem. B* **1998**, *102*, 5503; b) C.P. Jaroniec, R.K. Gilpin, M. Jaroniec, *J. Phys. Chem. B* **1997**, *101*, 6861.

[16] P. Innocenzi, H. Kozuka, T. Yoko, *J. Phys. Chem. B* **1997**, *101*, 2285.

[17] M. Stefanescu, M. Stoia, O. Stefanescu, *J. Sol-Gel Sci. Techn.* **2007**, *41*, 71.

[18] M. Ammam, E.B. Easton, *Sens. Actuators B* **2012**, *161*, 520.

[19] D.V. Leff, L. Brandt, J.R. Heath, *Langmuir* **1996**, *12*, 4723.

[20] B. Sahoo, S.K. Sahu, P. Pramanik, *J. Mol. Catal. B: Enzym.* **2011**, *69*, 95.

Received: ((will be filled in by the editorial staff))
Revised: ((will be filled in by the editorial staff))
Published online: ((will be filled in by the editorial staff))

Entry for the Table of Contents (Please choose one layout only)

Layout 1:

Janus nanoparticles based nanomachine

Reynaldo Villalonga, Paula Díez, Alfredo Sánchez, Elena Aznar, Ramón Martínez-Máñez, José M. Pingarrón*……..…… Page – Page*

Enzyme-controlled sensing-actuating nanomachine based on Janus Au-mesoporous silica nanoparticles

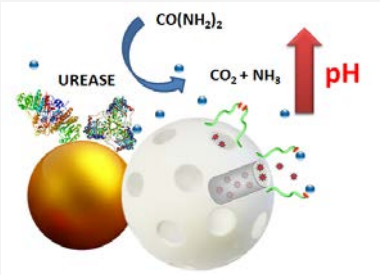

Integrated sensing-actuating nanomachine based on Janus Au-mesoporous silica nanoparticles with gate-like scaffolding for enzyme-controlled cargo release

Supporting Information

Enzyme-controlled sensing-actuating nanomachine based on Janus Au-mesoporous silica nanoparticles

Reynaldo Villalonga, Paula Díez, Alfredo Sánchez, Elena Aznar, Ramón Martínez-Máñez, José M. Pingarrón

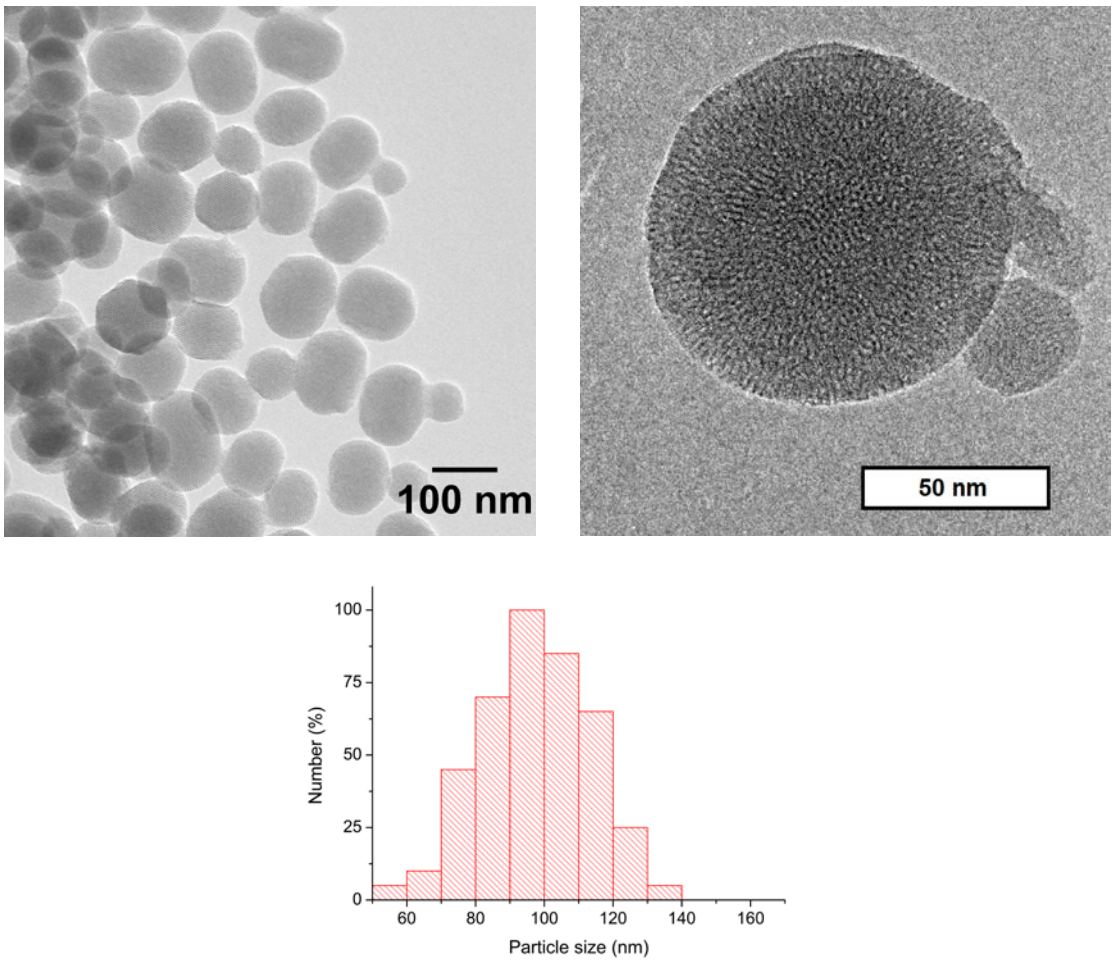

Figure 1S. TEM images and distribution of sizes of MS nanoparticles

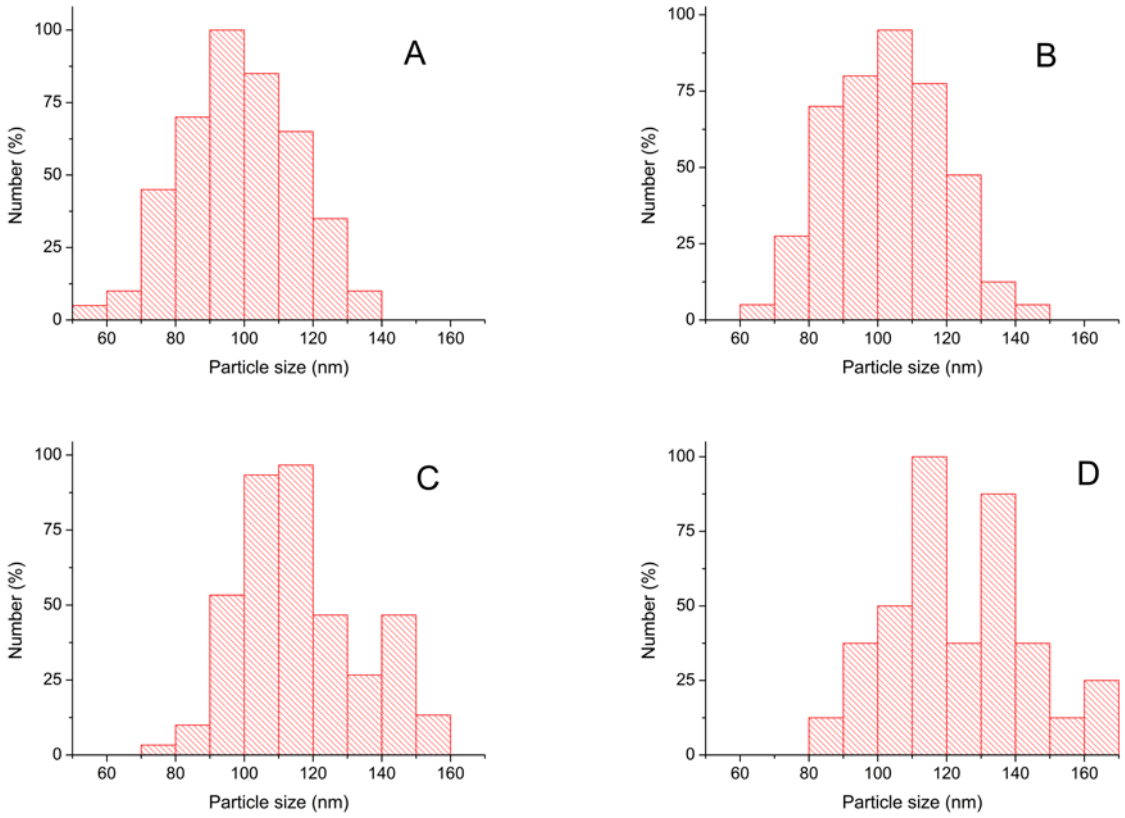

Figure 2S. Distribution of sizes of J1 (A), J2 (B), J3 (C) and J4 (D) nanoparticles

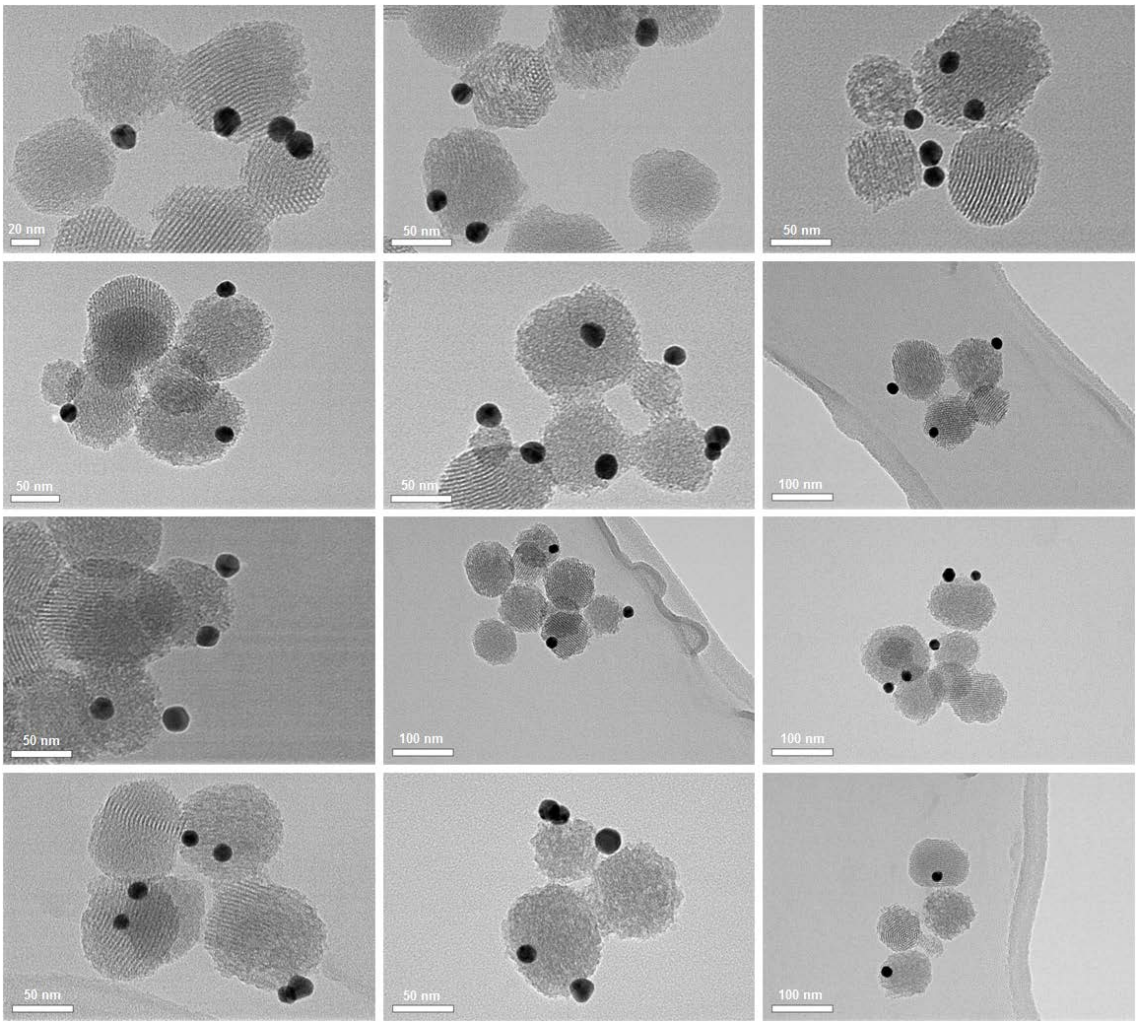

Figure 3S. TEM images of J2 nanoparticles.